RESEARCH ARTICLE

Aerodynamic performance of a ventilation system for droplet control by coughing in a hospital isolation ward

Yunfei Song[1] · Chengqing Yang[2] · Hui Li[1,3,4] · Hongbin Chen[5] · Shengnan Shen[4] · Yuqing Hou[1] · Jiayue Wang[1]

Abstract

Over 766 million people have been infected by coronavirus disease 2019 (COVID-19) in the past 3 years, resulting in 7 million deaths. The virus is primarily transmitted through droplets or aerosols produced by coughing, sneezing, and talking. A full-scale isolation ward in Wuhan Pulmonary Hospital is modeled in this work, and water droplet diffusion is simulated using computational fluid dynamics (CFD). In an isolation ward, a local exhaust ventilation system is intended to avoid cross-infection. The existence of a local exhaust system increases turbulent movement, leading to a complete breakup of the droplet cluster and improved droplet dispersion inside the ward. When the outlet negative pressure is 4.5 Pa, the number of moving droplets in the ward decreases by approximately 30% compared to the original ward. The local exhaust system could minimize the number of droplets evaporated in the ward; however, the formation of aerosols cannot be avoided. Furthermore, 60.83%, 62.04%, 61.03%, 60.22%, 62.97%, and 61.52% of droplets produced through coughing reached patients in six different scenarios. However, the local exhaust ventilation system has no apparent influence on the control of surface contamination. In this study, several suggestions with regards to the optimization of ventilation in wards and scientific evidence are provided to ensure the air quality of hospital isolation wards.

Keywords Computational fluid dynamics (CFD) · Virus airborne diffusion · Local exhaust ventilation system

Introduction

The study of airborne diseases has recently become increasingly significant with the emergence of severe acute respiratory syndrome, Ebola virus, tuberculosis, coronavirus disease 2019 (COVID-19), and other infectious diseases (Hathway et al. 2011). With the worldwide outbreak of COVID-19 (as of May 10, 2023), there have been 765,903,278 people diagnosed with COVID-19, including 6,927,378 deaths globally (WTO 2023). Some countries or regions succeeded in preventing the spread of the epidemic by managing quarantines and closures, which seriously affected economic growth and the normal operation of whole cities. Over the last 3 years, countries have prioritized preventing and controlling the epidemic. At the beginning of the outbreak, 100,000 people died every day worldwide as a result of COVID-19. It can affect anyone anywhere, especially healthcare workers exposed to environmental existing virus droplets. Therefore, the study of airborne virus diffusion in hospital isolation rooms is significant.

Viral respiratory infections are diffused by contact and droplet transmission, fomite transmission, and other types of transmission (WTO 2020). Contact transmission occurs when a healthy man is in close contact with an infected person (direct contact) or when an infected individual exhausts fomites containing viral droplets (indirect contact) (Morawska and Cao 2020). Viruses spread through the air via droplets or aerosols produced during coughing, sneezing, and talking (Jones and Brosseau 2015). Coughing, which is an

✉ Hui Li
li_hui@whu.edu.cn

[1] The Institute of Technological Sciences, Wuhan University, Wuhan 430072, China

[2] Wuhan Pulmonary Hospital, Wuhan Institute for Tuberculosis Control, Wuhan 430030, China

[3] Key Laboratory of Hydraulic Machinery Transients (Wuhan University), Ministry of Education, Wuhan 430072, China

[4] School of Power and Mechanical Engineering, Wuhan University, Wuhan 430072, China

[5] Pulmonary and Critical Care Medicine, Renmin Hospital of Wuhan University, Wuhan 430060, China

intense process of droplet generation over transient time, has recently been the focus of many studies. Small virus droplets expelled into the air can exist as airborne droplets for a long time (Chartier et al. 2009) and can fill the whole room under the effect of an air conditioner (Liu et al. 2020b). Li et al. 2020a, b) investigated the spread of droplets in a tropical outdoor environment and found that at wind speeds of 2 m/s, 100 μm droplets can move up to 6.6 m. Wei and Li (2015) modeled the coughing process as a turbulence jet to investigate the diffusion of droplets and obtained travel distances with different droplet sizes. Lindsley et al. (2016) compared aerosol droplet samples of 61 adult volunteer outpatients through experiments and found that more aerosol droplets containing viruses were released through coughing. Nicas et al. (2005) analyzed pathogen-containing droplet emissions from an infected person, and the results indicated that the droplets were composed of 98.2% water and 1.8% nonvolatile solid compounds. Besides, after exhaling infectious droplets through cough, small suspended droplets can form short-duration droplet clouds (Kukkonen et al. 1989; Mao et al. 2020). Then, droplets could be suspended via air in the ward for a long time. The surface of the droplet exchanges much heat and mass with the ambient environment (Parienta et al. 2011; Chao and Wan 2006). In other words, a portion of the droplets evaporates into water vapor suspended indoors for a long time. Therefore, the evaporation process of the suspension droplets is of great significance in analyzing the risk of infectious droplet transmission.

Furthermore, the COVID-19 outbreak can spread from one room to another via ventilation systems. Nissen et al. (2020) investigated the ventilation system in a COVID-19 isolation unit at Uppsala University Hospital through an experiment. They found that the virus could spread long distances via central ventilation systems. Other researchers have also found viral RNA in samples from ventilation systems in isolation rooms (Guo et al. 2020; Liu et al. 2020a, b). Thus, long distance airborne dispersal of the COVID-19 virus in hospital wards exists and significantly increases cross-infection risk.

Computational fluid dynamics (CFD) has been widely utilized to analyze the mobility of droplets indoors. Davardoost and Kahforoushan (2019) simulated the dispersion of volatile organic compounds indoors via CFD modeling to investigate the performance of ventilation. Liu et al. (2020a, b) used a full-experimental and numerical simulation to investigate the transmission and deposition of bioaerosols in a hospital isolation ward in which the renormalization group (RNG) k-ε model was selected. Bhattacharyya et al. (2020) studied the flow field in an isolation ward when both an air-conditioning system and a sanitizing machine continued working during the CFD simulation in which the transition SST k-ε model was applied. They found that the highly turbulent fields generated in the ward may be

conducive to the spread of sanitizers. Borro et al. (2020) used the CFD method to investigate droplet diffusion from a coughing event in the waiting room and recovery ward of Vatican State Children's Hospital, and the RNG k-ε model was employed in numerical simulation. The results indicated that the ventilation system accelerated the spread of infected droplets across the whole waiting room and that the local exhaust ventilation system could help to remove the contaminated air. Li et al. (2020a, b) investigated the diffusion of droplets generated from the wound of a patient under four different ventilation systems during surgery through the CFD method and obtained the optimal arrangement of the ventilation system. Cho (2018) evaluated the flow field of contaminated droplets exhaled from patients in an isolation ward at three different ventilation systems and obtained an improved ventilation system using numerical simulation and field measurement, which efficiently removed contaminated droplets.

Although extensive studies have been conducted on the simulation of droplet dispersion from a coughing episode and contaminant dispersal throughout the ward, little research has been performed with regard to the fast removal of contamination sources in an isolation ward. The main objective of this work is to analyze the propagation characteristics of droplets containing viruses induced by coughing in a ward and to design a local exhaust ventilation system to control droplet diffusion. A full-scale experiment is conducted to verify the flow field. The temporal and spatial distributions of droplets in six scenarios are simulated through the CFD method. Additionally, the number of moving, evaporated, and deposited droplets is quantitatively analyzed. This study provides several guidelines for optimizing ventilation in hospital wards and scientific evidence for ensuring the air quality of hospital isolation wards.

Problem description

The main transmission route of infection is that viruses spread through the air via droplets or aerosols produced during coughing, sneezing, and talking (Jones and Brosseau 2015). A high concentration of contaminated droplets in the hospital epidemic ward increases the danger of infection from patients to healthcare staff as well as patient cross-infection. A ventilation system ensures indoor air quality and protects healthcare workers and patients from contaminants (Liu et al. 2020a, b). Therefore, it is important to design an effective ventilation system to reduce droplet diffusion in hospital wards. Based on the above questions, coughing and droplet release processes in the isolation ward of Wuhan Pulmonary Hospital are simulated by using the CFD method to improve the performance of the ventilation system. The geometric model is established based on the actual

measurement of the isolation ward in Wuhan Pulmonary Hospital, as shown in Fig. 1.

According to Zhu et al. (2020), Yao et al. (2020), and Ke et al. (2020), COVID-19 is an enveloped virus with a large nucleoprotein, and virions ranging in size from 60 to 140 nm. Furthermore, Bi et al. (2022) discovered that the diameter of cough followed the Rosin–Rammler distribution, with an average diameter of 0.02 mm. Compared with the size of droplets, the size of virions can be ignored since they are tiny. We assume that all droplets contain viral droplets to simplify the model in the simulation. The material of droplets is simplified as water according to the investigation of Nicas et al. (2005). The droplets are injected from the mouth of a patient in the time range of 0.042–0.136 s, and the cough velocity can reach 22.06 m/s in a short period (Borro et al. 2020; Gupta et al. 2011), as shown in Fig. 2. And the evaporation process of the suspension droplets is considered in this work. The droplet properties used in the simulation are shown in Table 1.

Method

Geometry and mesh

The geometric model is established based on the actual measurement of the isolation ward in Wuhan Pulmonary Hospital. Some necessary simplifications with regards to the geometry of patients are made to reduce the computational cost. There is a naturally ventilated air outlet near the bed and a ventilation system located on the ceiling delivers fresh air to the ward. The patient is placed in the middle bed in this model. Figure 3 plots the schematic of the ward and the dimensions of the furniture.
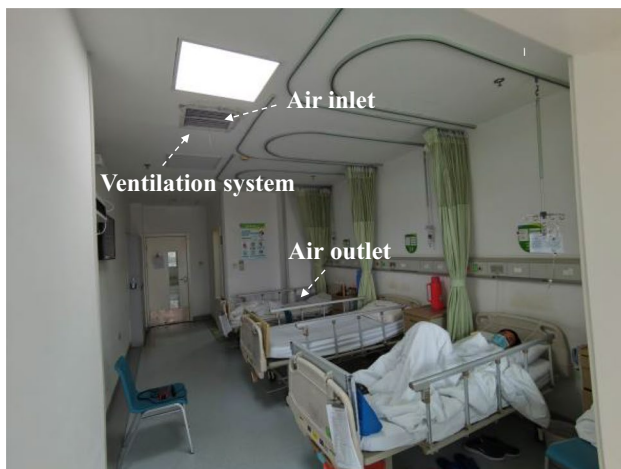
Fig. 1 Layout of an isolation ward in Wuhan Pulmonary Hospital

v_{top}=22.06 m/s
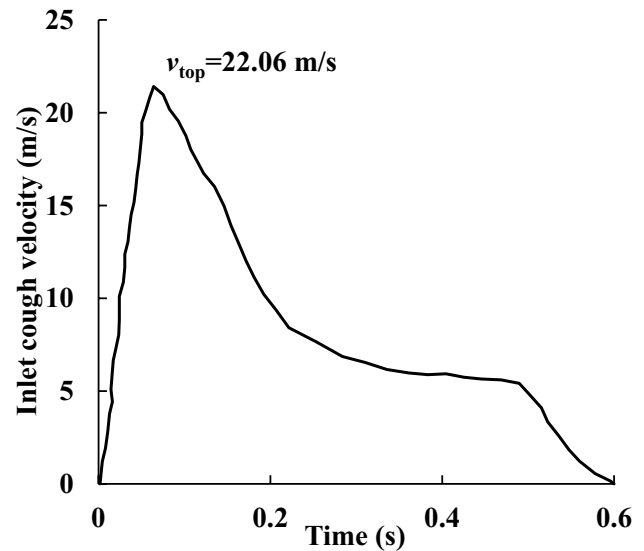
Fig. 2 Velocity profile of one cough by patient [13]

The meshes are generated using Gambit (ANSYS, Gambit 2.4.6, Canonsburg, PA, USA). The hybrid grid method is used in the gridding drawing process. The meshes of the furniture zone are generated using tetrahedron elements to ensure the quality of the mesh, which is shown in Fig. 4(a). Furthermore, the structured grid is used in the regular fluid zone to reduce the amount of calculation. Therefore, the meshes surrounding the patient are defined as plotted in Fig. 4(b) and (c) from the cross-sections of M-M and N–N, respectively. The whole zone of fluid consists of 5,807,108 tetrahedral and hexahedral elements. In our previous work (Cai et al. 2016; Zhang et al. 2015; Song et al. 2021), the same method was used to generate the mesh of the model. Thus, the validity of the mesh has already been verified.

Time step independence verification

To ensure the optimal configuration of the calculation accuracy and reliability in this work, time step independence verification is performed, as shown in Fig. 5. The air velocity at point P1 in Fig. 3 is used as a reference. Time step of 0.0005 s, 0.001 s, and 0.01 s are adopted for verification. Figure 5 indicates that the mean relative error is approximately 2.67% for a time step of 0.01 s while it is

Table 1 Droplets properties used in discrete phase model (Nicas et al. 2005; Borro et al. 2020; Gupta et al. 2011)

Material	Diameter distribution	Diameter (mm)	Velocity (m/s)	Temperature (K)
H_2O	Rosin–Rammler	0.002–0.1	22.06	310

Fig. 3 Schematic of the ward and the dimension of furniture (unit: mm)
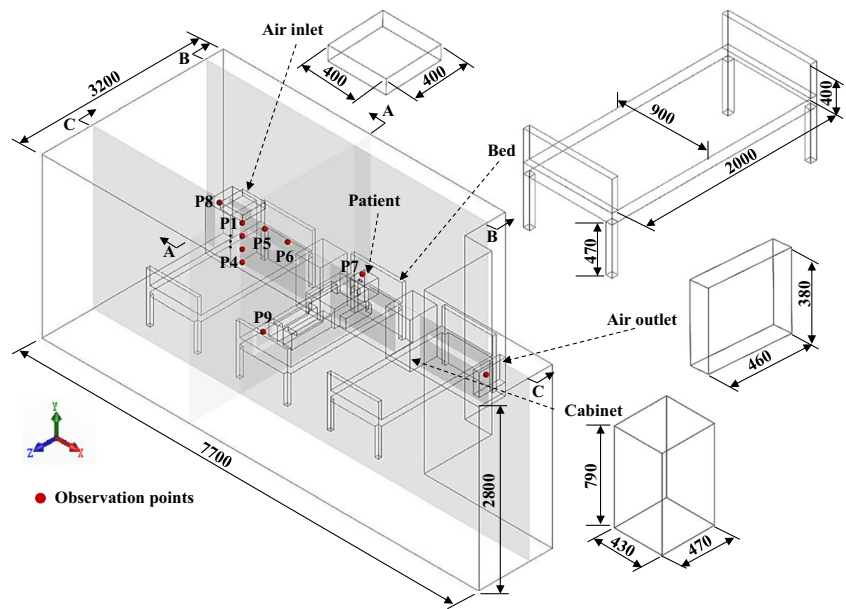
Fig. 4 Meshes for the CFD simulation **a** mesh of the furniture, **b** mesh of the manikin on the cross-section M-M, **c** mesh of the manikin on the cross-section N–N
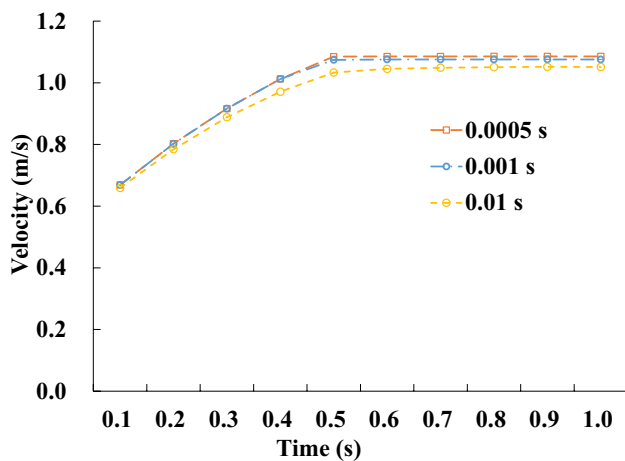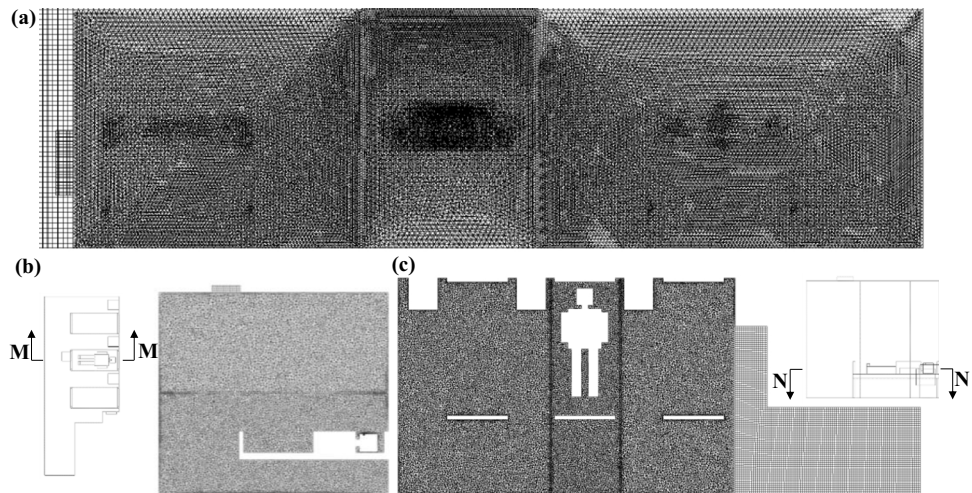
Fig. 5 Time step independence verification

approximately 0.57% for a time step of 0.0005 s when compared with the calculation result obtained with a time step of 0.001 s. To ensure accuracy and computational efficiency, a time step of 0.001 s is selected in further simulation.

Airflow modeling

The flow field is simulated using the CFD solver ANSYS Fluent (Fluent 2020 R2, ANSYS, Canonsburg, PA, USA). To simulate the indoor turbulence flow field, three turbulence models are extensively used: Reynolds average Navier–Stokes (RANS), direct numerical simulation (DNS), and large eddy simulation (LES) (Choi and Edwards 2012; Wang et al. 2018). In the indoor flow field simulation, the DNS and LES require longer computation times and more computer capacity than the RANS. Considering the accuracy

and amount of the calculation, the RANS equations are used (Chen 1995).

The continuity and the Navier–Stokes equation can be written as follows:

$$\frac{\partial \overline{u}_m}{\partial x_m} = 0 \tag{1}$$

$$\frac{\partial u_m}{\partial t} + \frac{\partial \left(\overline{u}_m \overline{u}_n \right)}{\partial \overline{u}_n} = -\frac{1}{\rho} \frac{\partial \overline{P}}{\partial x_m} + v \frac{\partial^2 \overline{u}_m}{\partial x_n x_n} + \frac{\partial \tau_{mn}}{\partial x_n} \tag{2}$$

where u_m is the fluid velocity in the m direction, x_m is the coordinate in the m direction, and P represents the pressure of the fluid. The overbar in the equations denotes the mean variables. Moreover, τ_{mn} represents the Reynolds stress.

A turbulent jet event (Bourouiba et al. 2014) can be used to simulate coughing; thus, the RNG k-ε model in the RANS method is used in the simulation, which has been proven effective in the simulation of indoor turbulent flow fields (Liu et al. 2020a, b; Borro et al. 2020; Liu et al. 2017). This model is derived from renormalization theory, in which an additional term is added to the epsilon equation to improve the accuracy of turbulence flow (Abraham and Magi 1997; Yakhot and Orszag 1986). Regarding the solving method, the pressure-implicit with the splitting of operators algorithm is selected due to its suitability for transient flows.

Discrete phase

To simulate the diffusion of droplets from a cough, a discrete model is used. The droplet force balance equation in the discrete phase model theory is defined as (Fluent ANSYS 2020)

$$m_d \frac{d\overline{u}_d}{dt} = m_d \frac{\overline{u}_f - \overline{u}_d}{\tau_r} + \frac{m_d \vec{g}(\rho_d - \rho)}{\rho_d} + \vec{F} \tag{3}$$

where m_d represents the mass of the droplet, $\vec{u}_f$ is the velocity of the fluid, $\vec{u}_d$ is the velocity of a droplet, $\vec{F}$ is an additional force, and τ_r is the relaxation time of a droplet.

In the right-hand side of the equation, the first term is the drag force; the second part represents a force under the influence of gravity; and the third part is additional forces under various circumstances, such as forces in moving reference frames, thermophoretic force, Brownian force, Saffman's lift force, Magnus lift force, and user-defined force.

Drag force and gravity have the greatest influence on the dynamic behavior of droplets formed by cough occurrences. The droplet motion is assumed to be a stochastic collision. Other forces, including thermophoresis and Brownian forces, are too small and are ignored in the simulation. Therefore, droplets are mainly affected by the drag forces, generation of turbulence associated with the ventilation system, and gravity.

The discrete model in this work is based on the work proposed by Borro et al (2020). They used the CFD method to investigate droplet diffusion from a coughing event in the waiting room and recovery ward of Vatican State Children's Hospital. The droplets are injected from the mouth of the patient in the time range of 0.042–0.136 s, and the cough velocity can reach 22.06 m/s in a short period. This work tries to control the number of droplets evaporated in the ward and the formation of aerosols by designing a local exhaust system.

Boundary condition

Before the simulation is performed, the inlet speed of the ventilation system is tested at Wuhan Pulmonary Hospital, and the speed obtained is 1.045 m/s. The air temperature is set to 295 K, and the walls are assumed to be adiabatic. Droplets are expected to be absorbed by surfaces (beds, cabinets, walls, and patients) as they collide with the surfaces due to their low momentum. Therefore, we select the trap as the boundary condition of the surfaces. The other boundary conditions for CFD simulation are summarized in Table 2.

Results and discussion

Validation of the flow field

In this study, the flow field and droplet diffusion in an isolation ward are investigated. Before conducting transient simulations, a stable scenario is simulated without considering coughing as the initial value to assure airflow stability in the room. The CFD simulation results in the isolation ward are plotted below. Figure 6 shows streamlines formed by the ventilation system of the isolation ward. As shown in Fig. 6(a), the airflow from the inlet impacts the flow field in the isolation room. After the airflow reaches the floor, one part of the airflow moves up the wall to the ceiling and forms a backflow zone, while the other part moves towards the empty area and returns. After the vertical air reaches the floor, the airflow hits the bed and produces a recirculation region. Figure 6(b) indicates the flow field on the cross-section of B-B. The airflow in the zone is observed to move towards the outlet, and a portion of the air reaches the furniture and forms an eddy current area. Figure 6(c) shows the flow field on the cross-section of C–C. After the air is delivered to the floor, the split flow reaches the floor and forms a backflow.

An experiment is conducted to measure the velocities of 10 points to verify the flow field simulation. The measuring apparatus (Hot ball anemometer WS-40, Hongrui, China) is selected for measurement, and placed in different positions

Table 2 Boundary conditions in the CFD simulation

	Original	Ventilation_1	Ventilation_2	Ventilation_3	Ventilation_4	Ventilation_5
Ventilation outlet	/	Outlet pressure (Pa)				
		−2.5	−3.0	−3.5	−4.0	−4.5
		Outlet temperature: 300 K				
		DPM condition: Escape				
Air inlet		Inlet velocity: 1.045 m/s				
		Inlet temperature: 295 K				
		DPM condition: Escape				
Air outlet		Outlet pressure: zero-gauge pressure				
		Outlet temperature: 300 K				
		DPM condition: Escape				
Droplet inlet		Droplet velocity: 22.06 m/s (in Y direction)				
		Droplet density: 997 kg/m^3				
		Droplet mass flow rate: 0.018 kg/s				
		Temperature: 310 K				
		DPM condition: Escape				
Surfaces (beds, cabinets, walls, and patient)		Temperature: 300 K				
		DPM condition: Trap				

Fig. 6 Flow fields on the cross-sections **a** A-A, **b** B-B, and **c** C–C
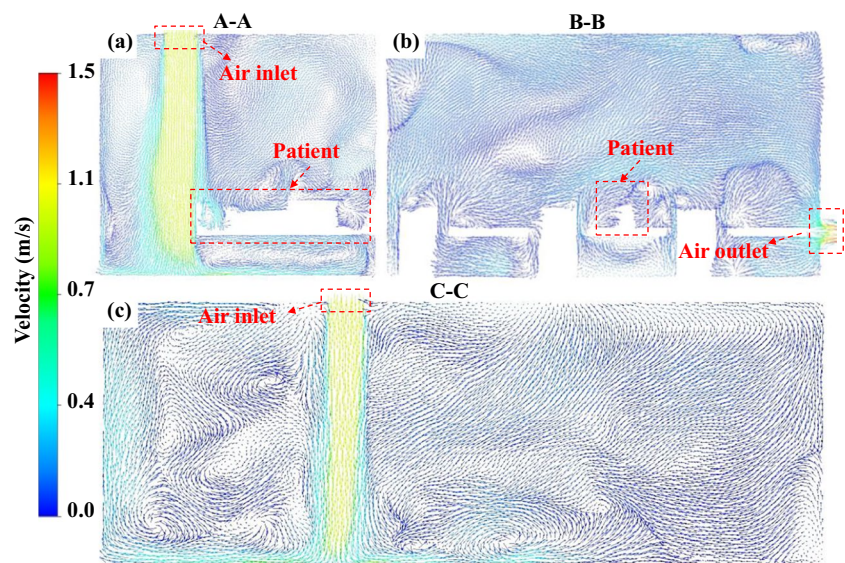
to measure the velocity. The locations of the observation points are illustrated in Fig. 2. And the parameters of WS-40 are summarized in Table 3. The test data can be collected in real-time and output to the laptop, as shown in Fig. 7.

During the experiment, the ventilation system is continuously operating. Furthermore, doors and windows are closed to separate the space from the outside. During the experiment, only the air conditioning is turned on, resulting in no temperature change.

The velocity validation results at selected points are shown in Fig. 8. The results of the experiment and simulation are consistent. The mean absolute percentage error is less than 10%, indicating that the boundary conditions of the CFD simulation are suitable. Because the actual airflow is turbulent, using anemometers to measure velocity is difficult. In addition, the simulation is simplified to lower the computing cost. Thus, certain errors will occur. However, in this model, the errors between the simulation and the experiment are acceptable.

Table 3 Parameters of hot-bulb anemometer

	Operating voltage	Temperature stability	Measurement range	Accuracy
	3.7 V	0~50℃	0~2 m/s	0.01 m/s

Fig. 7 Real-time acquisition of experiment data
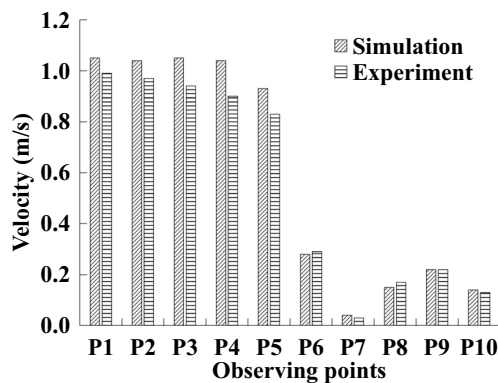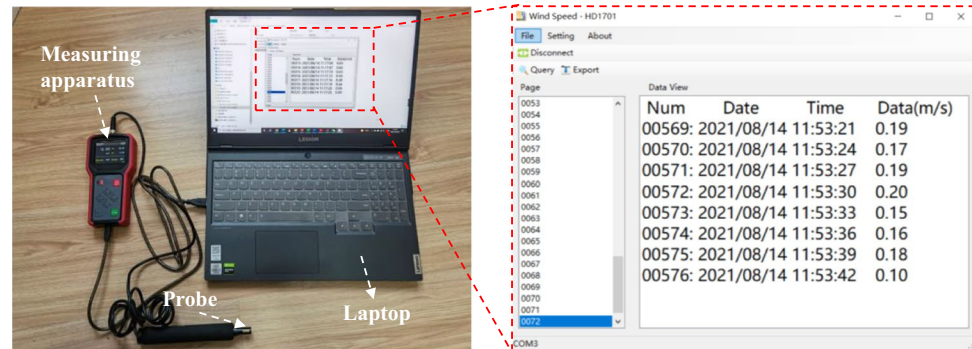
Fig. 8 Velocity validation at selected points

Diffusion and distribution of droplets

To investigate droplet diffusion in the isolation ward, a steady scenario is simulated without considering coughing to ensure airflow stability in the room before releasing droplets. When the flow field in the room stabilizes, droplets begin to be released (which means the patient starts coughing), and at this time $t = 0$ s. Figure 9 plots the temporal and spatial distributions of the droplets in the ward of Wuhan Pulmonary Hospital. At 0.1 s, a small portion is diffused to the exhaust under the action of the flow field, which can be seen in Fig. 9; moreover, most droplets gather to form a droplet cloud. Droplets disperse gradually because of the vortex around the patient. These droplets hit the ceiling and continue to move along the wall, which can be observed at

0.3–2.0 s in Fig. 9. Droplets begin to spread to the entire room at 3.0 s, affected by the eddy and buoyancy.

From the simulation results, the droplet movement is mainly influenced by the turbulence generated by the ventilation system in the ward. After the droplet is ejected from the mouth of a patient at the beginning, part of it moves upwards along the mainstream, and part of it is influenced by the vortex inside the room to be carried in unpredictable directions. Most droplets are eventually deposited on the patient's surface and the walls, and a small portion can be observed to spread in the ward, which could carry various and suspend indoors for a long time. To effectively prevent the spread of droplets in an isolation ward, a ventilation system must be designed to minimize turbulence and promote the effective removal of droplets through local exhaust ventilation system. Therefore, the local exhaust system is considered in the following work.

Local exhaust ventilation system

Droplets containing viruses may remain in rooms for a long time. Negative pressure ventilation systems isolate pathogenic droplets in hospitals, such as Wuhan Leishenshan Hospital (Luo et al. 2020). The layout of negative pressure wards can also minimize the exposure of patients and health care professionals to COVID-19 (Al-Benna 2021). According to the US Ventilation of Health Care Facilities, the minimum differential pressure between wards and relatively clean areas is 2.5 Pa (Rousseau and Sheerin 2017). A local exhaust ventilation system, which is placed above the head of a patient, is designed to ensure the air quality of the
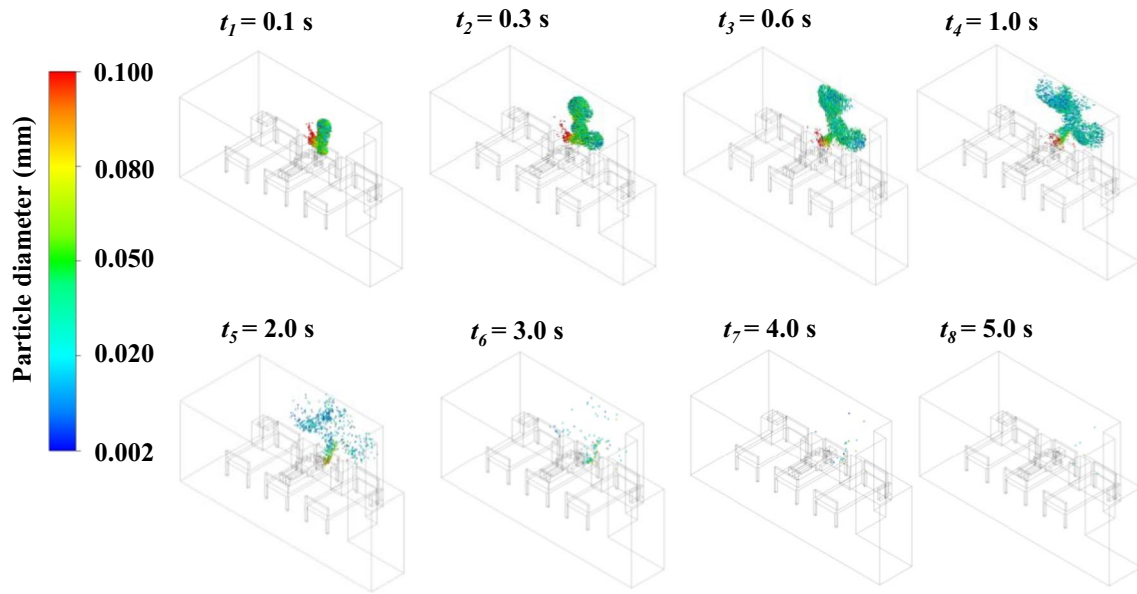
Fig. 9 Temporal and spatial distributions of droplets in the original ward

isolation ward. The geometry of the ward furnished with the ventilation system and the dimensions of the system are shown in Fig. 10.

The initial outlet negative pressure of the local exhaust ventilation system is set to 2.5 Pa in scenario Ventilation_1, and the other boundary conditions for CFD simulation are summarized in Table 2. The purpose of the simulation is to analyze the effect of the local exhaust system on droplet diffusion.

The temporal and spatial distributions of droplets in the ward furnished with a local exhaust ventilation system are plotted in Fig. 11. Interestingly, the existence of the local exhaust system promotes turbulent transport around the head of the patient, leading to a complete breakup of the droplet cluster and enhancement of indoor droplet dispersion. At 5.0 s, few droplets can be tracked moving in the ward, which indicates that most droplets are deposited or escape from the outlet. With an increase in the negative pressure, the

Fig. 10 Schematic of the isolation ward (unit: mm) furnished with the local exhaust ventilation system
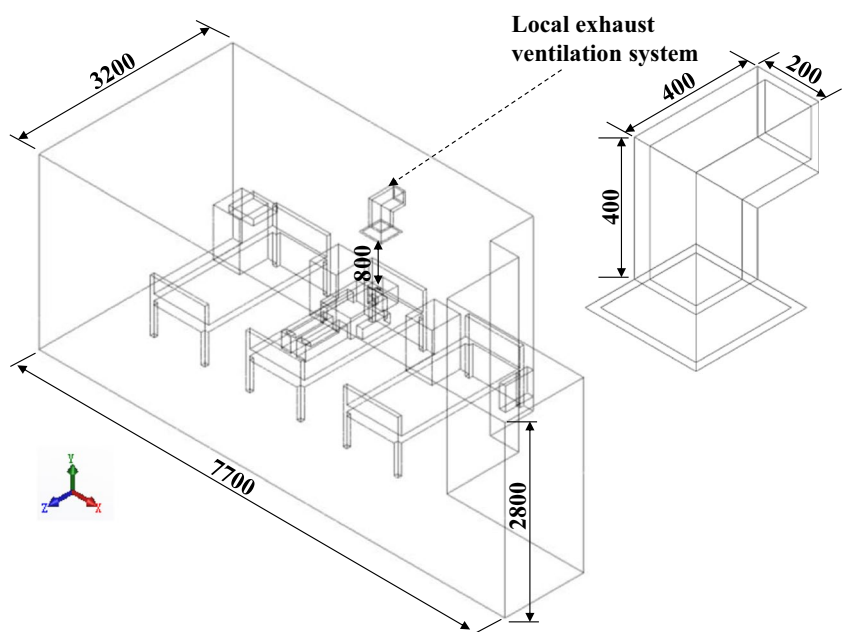
local exhaust ventilation system can exhaust more droplets containing pathogenic microorganisms.

When the local exhaust ventilation system is furnished in the ward, droplet movement is mainly influenced by the negative pressure caused by the local exhaust ventilation system. The negative pressure causes air to flow towards the exhaust outlet, which may carry droplets. As the air flows towards the outlet, it can create turbulence and vortices in the area around the outlet, which can cause droplets to disperse and become more evenly distributed throughout the room. However, the existence of the local exhaust ventilation system cannot remove all droplets thoroughly. Vortices can form in the area around the ventilation system, resulting in a portion of droplets contained in the room and moving with the indoor air. Increasing the negative pressure can enhance the effectiveness of the local exhaust system in removing droplets containing pathogenic microorganisms. However, there is a limit to the amount of negative pressure that can be applied because excessively high negative pressure can create too much turbulence and vortices in the room, which can actually hinder the effective removal of droplets.

To obtain the influence of the outlet negative pressure on droplet diffusion, two more scenarios, in which the outlet negative pressure is 4.0 (ventilation_4) and 4.5 Pa (ventilation_5), are considered. Moreover, we quantitatively analyze the droplet number at different moments in six scenarios. The results show that the local exhaust ventilation system can reduce the number of droplets, which can be seen in Fig. 12. When the negative outlet pressure is 2.5 Pa, 23.6% of droplets are produced through coughing tracked in the ward. The number of moving droplets in the ward decreases by nearly 15% compared with the original situation. Interestingly, as the negative outlet pressure rises from the initial value to 3.0 Pa, there are 24.5% of droplets produced through coughing tracked in the ward, which means that more droplets remain in the room than in the original ward. Thus, the existence of the local exhaust system promotes turbulent transport. This turbulence can lead to a complete disruption of the droplet cloud and an increase in the dispersion of droplets, which in turn can result in more droplets being tracked in the ward. As the outlet negative pressure increases, it is found that the number of droplets remaining in the room gradually decreases from 24.5 to 21.9%. When the negative outlet pressure increases to 4.5 Pa, the local exhaust ventilation system can capture and exhaust more droplets than in other scenarios. The number of droplets tracked in the ward was reduced by nearly 30% compared with the original ward. This is because the mass of the droplets is light, and when the negative outlet pressure value reaches a certain value, droplets caused by a coughing event can be removed more effectively.

In addition to the droplets that spread with the air in the ward, a portion of droplets evaporates into water vapor.

Figure 13 illustrates the number of droplets that evaporated in the ward over time. More droplets evaporate into water vapor and exist in the room in the form of water vapor over time, which is more conducive to the formation of aerosols. This allows pathogenic microorganisms to remain indoors for a long time, which increases the exposure of COVID-19 to health care staff. The local exhaust system can minimize the number of droplets evaporated in the ward. However, the formation of aerosols cannot be avoided.

Regarding the number of deposited droplets, 60.83%, 62.04%, 61.03%, 60.22%, 62.97%, and 61.52% of droplets produced through coughing were deposited on the area around the patient in the six scenarios. Figure 14 illustrates the number of droplets deposited on the surface of patient with different diameters. The number of droplets with diameters of 0.01–0.03 mm accounts for nearly 38.1% of the deposited droplets. According to the results, the local exhaust system has no obvious impact on the prevention and control of surface contamination. There are several factors that may contribute to the local exhaust system's limited effectiveness in preventing and controlling surface contamination. Firstly, the local exhaust system may not be capturing all of the contaminated droplets in the room, particularly if the exhaust rate is not sufficiently high. Additionally, the local exhaust system may not be able to effectively capture droplets that have settled on surfaces, particularly if they are located in areas that are difficult to access or shielded from the air flow.

According to the statistical results, we find that the droplets can be effectively removed to a certain extent when the negative pressure of the local ventilation system is 4.0 and 4.5 Pa. In other words, the optimal negative pressure value in this simulation is 4.0 or 4.5 Pa. However, the CFD model in this work may not be sufficient. Several factors, such as the location of the local exhaust system and the composition of the droplets, also need to be considered in future work. The goal is to obtain the optimal negative outlet pressure value that is sufficiently strong to remove droplets from the ward but not too strong that it creates discomfort for patients.

Conclusion

In this study, the full-scale geometry of the isolation ward in Wuhan Pulmonary Hospital is modeled, and the droplet diffusion process from a coughing event in the ward is simulated. An experiment is conducted to validate the CFD model, and a local exhaust ventilation system is designed to ensure indoor air quality.

(1) Although the local exhaust ventilation system reduces the number of airborne contaminants, a substantial increase in turbulent air motions may occur. The results
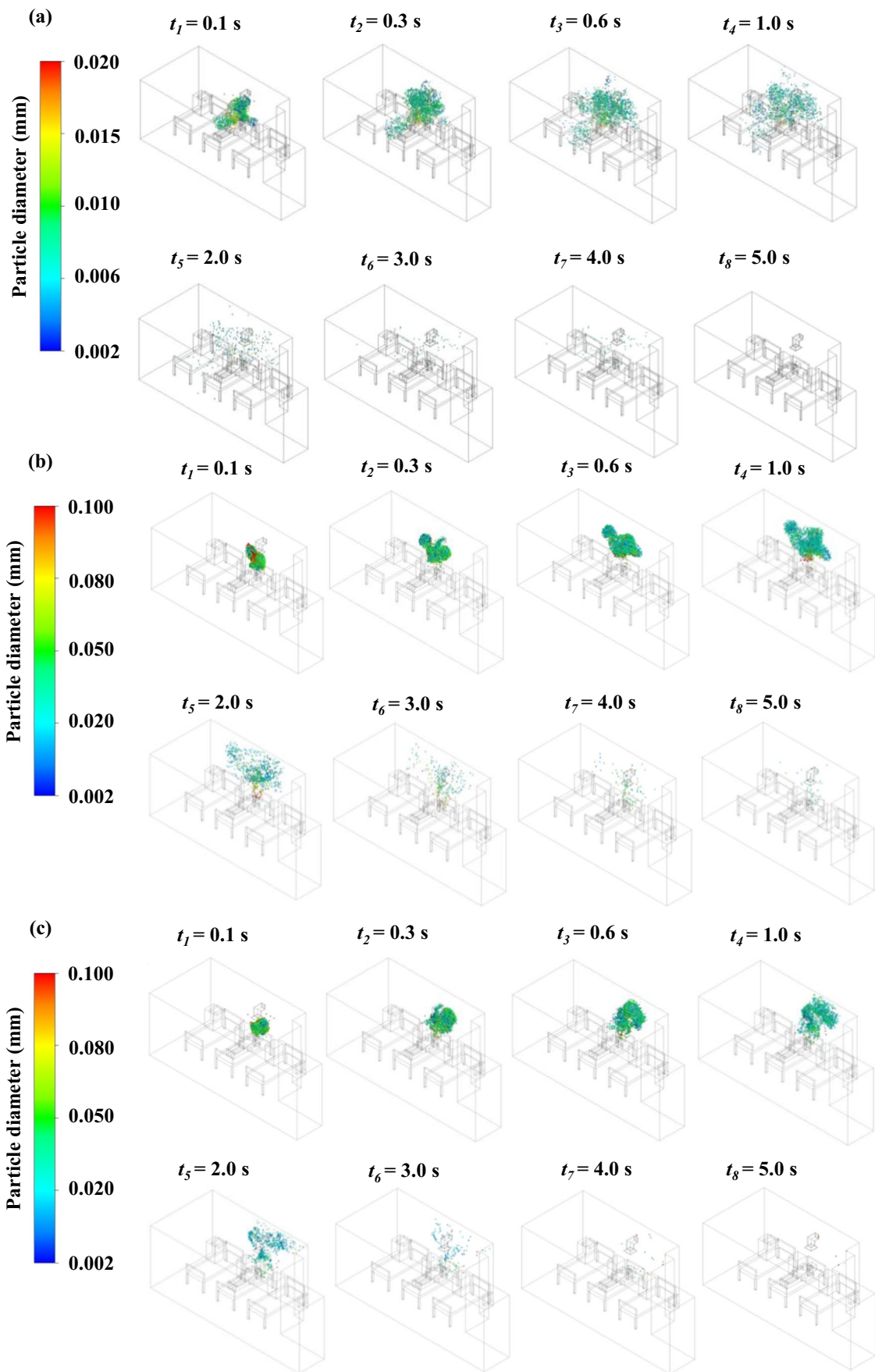
◀**Fig. 11** Temporal and spatial distributions of droplets with designed local exhaust ventilation system when outlet negative pressure is **a** 2.5 Pa, **b** 3.0 Pa, and **c** 3.5 Pa

Fig. 12 Number of droplets moving in the ward over time
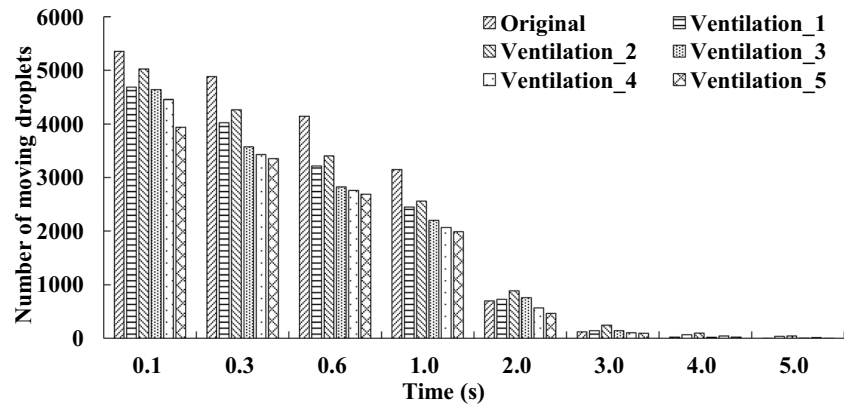
Fig. 13 Number of droplets evaporated in the ward over time
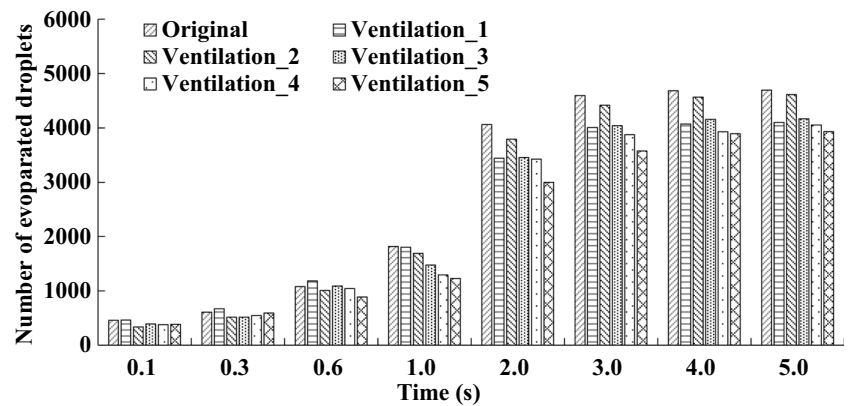
Fig. 14 Number of droplets deposited on the surface of the patient in the ward with different diameters
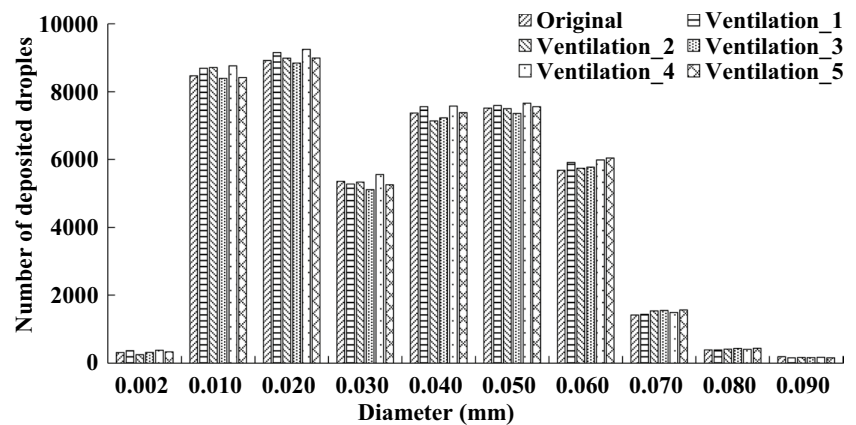
show that a negative outlet pressure of 2.5 and 3.5 Pa led to a decrease in evaporated droplets and airborne contaminants remaining indoors, and the negative outlet pressure of 3.0 Pa increases the number of droplets tracked in the ward of the excessively turbulent flow. It is found that the number of droplets remaining indoors on the outlet negative pressure is not linear. The exhaust system can effectively extract contaminants when the negative pressure value is small. However, the negative pressure is increased, and the local exhaust system promotes turbulent transport, leading to a complete breakup of the droplet cluster and enhancing the dispersion of droplets indoors. The mass of the droplets is light, and when the outlet negative pressure value reaches a certain value, droplets can also be effectively removed.

(2) The local exhaust system can minimize the number of droplets evaporated in the ward. However, the formation of aerosols cannot be avoided.

(3) Furthermore, 60.83%, 62.04%, 61.03%, 60.22%, 62.97%, and 61.52% of droplets produced through coughing are deposited on the surface of patient in six scenarios. According to the results, the local exhaust system has no obvious influence on the prevention and control of surface contamination.

Nevertheless, the simulation in the isolation ward proved that the local exhaust ventilation system reduces the number of airborne contaminants remaining indoors. However, the compound of the contaminant droplets is complicated to simulate in CFD, and the droplets are assumed to be absorbed on the surface when droplets collide with the surfaces. The spread of infectious diseases is complex. Therefore, it is difficult to simulate through the CFD method to restore the real process and the CFD model in this work may not be sufficient in providing a comprehensive analysis.

The significance of this work is to provide a detailed analysis of contaminant diffusion in the Wuhan Pulmonary Hospital isolation ward. This work can also provide guidelines for optimizing ventilation in hospital wards and constitutes scientific evidence for preserving air quality in isolation wards. In future work, we will focus on improving the CFD model to study the influence of the ventilation system on jet turbulence and further reduce the diffusion of contaminant droplets.

Declarations

References

Abraham J, Magi V (1997) Computations of transient jets: RNG k-ε model versus standard k-ε model. SAE Trans 1442–1452. https://doi.org/10.4271/970885

Al-Benna S (2021) Negative pressure rooms and COVID-19. J Perioper Pract 31(1–2):18–23. https://doi.org/10.1177/1750458920949453

Bhattacharyya S, Dey K, Paul AR, Biswas R (2020) A novel CFD analysis to minimize the spread of COVID-19 virus in hospital isolation room. Chaos Solitons Fractals 139:110294. https://doi.org/10.1016/j.chaos.2020.110294

Bi R, Ali S, Savory E, Zhang C (2022) A numerical modelling investigation of the development of a human cough jet. Eng Comput 39(2):773–791. https://doi.org/10.1108/EC-12-2020-0705

Borro L, Mazzei L, Raponi M et al (2020) The role of air conditioning in the diffusion of sars-cov-2 in indoor environments: a first computational fluid dynamic model, based on investigations performed at the Vatican state children's hospital. Environ Res 193:110343. https://doi.org/10.1016/j.envres.2020.110343

Bourouiba L, Dehandschoewercker E, Bush JWM (2014) Violent expiratory events: on coughing and sneezing. J Fluid Mech 745:537–563. https://doi.org/10.1017/jfm.2014.88

Cai M, Shen S, Li H et al (2016) Study of contact characteristics between a respirator and a head form. J Occup Environ Hyg 13(3):50–60. https://doi.org/10.1080/15459624.2015.1116699

Chao CY, Wan MP (2006) A study of the dispersion of expiratory aerosols in unidirectional downward and ceiling-return type airflows using a multiphase approach. Indoor Air 16(4):296–312. https://doi.org/10.1111/j.1600-0668.2006.00426.x

Chartier Y, Atkinson J, Pessoa-Silva C (2009) Natural ventilation for infection control in health-care settings. World Health Organization. Available online: https://www.ncbi.nlm.nih.gov/books/NBK143284/. Accessed Jan 2009

Chen Q (1995) Comparison of different k-ε models for indoor air flow computations. Numer Heat Tr B-Fund 28(3):353–369. https://doi.org/10.1080/10407799508928838

Cho J (2018) Investigation on the contaminant distribution with improved ventilation system in hospital isolation rooms: effect of supply and exhaust air diffuser configurations. Appl Therm Eng 148:208–218. https://doi.org/10.1016/j.applthermaleng.2018.11.023

Choi JI, Edwards JR (2012) Large-eddy simulation of human-induced contaminant transport in room compartments. Indoor Air 22(1):77–87. https://doi.org/10.1111/j.16000668.2011.00741.x

Davardoost F, Kahforoushan D (2019) Evaluation and investigation of the effects of ventilation layout, rate, and room temperature on pollution dispersion across a laboratory indoor environment.

Environ Sci Pollut Res 26(6):5410–5421. https://doi.org/10.1007/s11356-018-3977-8

Fluent ANSYS (2020) Fluent 2020 R2 user guide. ANSYS Fluent, Canonsburg. Available online https://ansyshelp.ansys.com/account/secured?returnurl=/Views/Secured/corp/v231/en/flu_ug/pt03.html. Accessed 15 May 2023

Guo ZD, Wang ZY, Zhang SF et al (2020) Aerosol and surface distribution of severe acute respiratory syndrome coronavirus 2 in hospital wards, Wuhan, China, 2020. Emerging Infect Dis 26(7):1586. https://doi.org/10.3201/eid2607.200885

Gupta JK, Lin CH, Chen Q (2011) Transport of expiratory droplets in an aircraft cabin. Indoor Air 21(1):3–11. https://doi.org/10.1111/j.1600-0668.2010.00676.x

Hathway EA, Noakes CJ, Sleigh PA, Fletcher LA (2011) CFD simulation of airborne pathogen transport due to human activities. Build Environ 46(12):2500–2511. https://doi.org/10.1016/j.buildenv.2011.06.001

Jones RM, Brosseau LM (2015) Aerosol transmission of infectious disease. J Occup Environ Med 57(5):501–508. https://doi.org/10.1097/JOM.0000000000000448

Ke Z, Oton J, Qu K et al (2020) Structures and distributions of SARS-CoV-2 spike proteins on intact virions. Nature 588(7838):498–502. https://doi.org/10.1038/s41586-020-2665-2

Kukkonen J, Vesala T, Kulmala M (1989) The interdependence of evaporation and settling for airborne freely falling droplets. J Aerosol Sci 20(7):749–763. https://doi.org/10.1016/0021-8502(89)90087-6

Li H, Leong FY, Xu G et al (2020) Dispersion of evaporating cough droplets in tropical outdoor environment. Phys Fluids 32(11):113301. https://doi.org/10.1063/5.0026360

Li H, Zhong K, Zhai Z (John) (2020) Investigating the influences of ventilation on the fate of particles generated by patient and medical staff in operating room. Build Environ 180:107038. https://doi.org/10.1016/j.buildenv.2020.107038

Lindsley WG, Blachere FM, Beezhold DH et al (2016) Viable influenza a virus in airborne particles expelled during coughs versus exhalations. Influenza Other Respir Viruses 10(5):404–413. https://doi.org/10.1111/irv.12390

Liu Y, Li H, Feng G (2017) Simulation of inhalable aerosol particle distribution generated from cooking by Eulerian approach with RNG k–epsilon turbulence model and pollution exposure in a residential kitchen space. Build Simul 10:135–144. https://doi.org/10.1007/s12273-016-0313-4

Liu Y, Ning Z, Chen Y et al (2020) Aerodynamic analysis of SARS-CoV-2 in two Wuhan hospitals. Nature 582(7813):557–560. https://doi.org/10.1038/s41586-020-2271-3

Liu Z, Wang L, Rong R et al (2020) Full-scale experimental and numerical study of bioaerosol characteristics against cross-infection in a two-bed hospital ward. Build Environ 186:107373. https://doi.org/10.1016/j.buildenv.2020.107373

Luo H, Liu J, Li C et al (2020) Ultra-rapid delivery of specialty field hospitals to combat COVID-19: lessons learned from the Leishenshan Hospital project in Wuhan. Autom Constr 119:103345. https://doi.org/10.1016/j.autcon.2020.103345

Mao N, An CK, Guo LY et al (2020) Transmission risk of infectious droplets in physical spreading process at different times: a review. Build Environ 185:107307. https://doi.org/10.1016/j.buildenv.2020.107307

Morawska L, Cao J (2020) Airborne transmission of SARS-CoV-2: the world should face the reality. Environ Int 139:105730. https://doi.org/10.1016/j.envint.2020.105730

Nicas M, Nazaroff WW, Hubbard A (2005) Toward understanding the risk of secondary airborne infection: emission of respirable pathogens. J Occup Environ Hyg 2(3):143–154. https://doi.org/10.1080/15459620590918466

Nissen K, Krambrich J, Akaberi D et al (2020) Long-distance airborne dispersal of SARS-CoV-2 in COVID-19 wards. Sci Rep 10(1):1–9. https://doi.org/10.21203/rs.3.rs-34643/v1

Parienta D, Morawska L, Johnson GR et al (2011) Theoretical analysis of the motion and evaporation of exhaled respiratory droplets of mixed composition. J Aerosol Sci 42(1):1–10. https://doi.org/10.1016/j.jaerosci.2010.10.005

Rousseau CP, Sheerin MP (2017) ANSI/ASHRAE/ASHE Standard 170-2017 Ventilation Standard For Health Care Facilities. Available online: https://www.ashrae.org/. Accessed May 2023

Song Y, Yang Q, Li H et al (2021) Simulation of indoor cigarette smoke particles in a ventilated room. Air Qual Atmos Health 14(11):1837–1847. https://doi.org/10.1007/s11869-021-01057-z

Wang C, Holmberg S, Sadrizadeh S (2018) Numerical study of temperature-controlled airflow in comparison with turbulent mixing and laminar airflow for operating room ventilation. Build Environ 144:45–56. https://doi.org/10.1016/j.buildenv.2018.08.010

Wei J, Li Y (2015) Enhanced spread of expiratory droplets by turbulence in a cough jet. Build Environ 93:86–96. https://doi.org/10.1016/j.buildenv.2015.06.018

WTO (World Health Organization) (2020) Transmission of SARS-CoV-2: implications for infection prevention precautions. Available online: https://www.who.int/news-room/commentaries/detail. Accessed 14 Aug 2020

WTO (World Health Organization) (2023) WHO coronavirus (COVID-19) dashboard. Available online: https://covid19.who.int/. Accessed 10 May 2023

Yakhot V, Orszag SA (1986) Renormalization group analysis of turbulence. I Basic Theory J Sci Comput 1(1):3–51. https://doi.org/10.1007/BF01061452

Yao H, Song Y, Chen Y et al (2020) Molecular architecture of the SARS-CoV-2 virus. Cell 183(3):730–738. https://doi.org/10.37473/dac/10.1101/2020.04

Zhang X, Li H, Shen S, Cai M (2015) Investigation of the flow-field in the upper respiratory system when wearing N95 filtering facepiece respirator. J Occup Environ Hyg 13(5):372–382. https://doi.org/10.1080/15459624.2015.1116697

Zhu N, Zhang D, Wang W et al (2020) A novel coronavirus from patients with pneumonia in China, 2019. N Engl J Med 382(8):727–733. https://doi.org/10.37473/dac/10.1101/2020.04.07.20057299